

# A Fluorescence Nanosensor for Glycoproteins with Activity Based on the Molecularly Imprinted Spatial Structure of the Target and Boronate Affinity\*\*

Wei Zhang, Wei Liu, Ping Li,\* Haibin Xiao, Hui Wang, and Bo Tang\*

**Abstract:** Glycoproteins are closely associated with the occurrence of diverse diseases, and they have been used as biomarkers and therapeutic targets in clinical diagnostics. Currently, mass spectrometry has proven to be a powerful tool for glycoprotein analysis, but it is almost impossible to directly identify glycoproteins without the preparation and pretreatment of samples. Furthermore, biological samples, especially proteins, are damaged by this process. Herein, we describe a novel fluorescence nanosensor based on a molecularly imprinted spatial structure and boronate affinity that is well-suited for monitoring glycoproteins selectively. Results showed that the recognition performance of the nanosensor for glycoproteins was regulated by controlling the pH value and temperature. Moreover, the nanosensor was successfully applied to the detection of HRP in biological fluids. This study provides a facile and efficient fluorescence tool for glycoprotein detection in clinical diagnostics.

Glycoproteins are a large family of proteins that play important roles in numerous biological events. They have been used as biomarkers and therapeutic targets in clinical diagnostics.<sup>[1]</sup> Mass spectrometry has proven to be a powerful tool for glycoprotein analysis, but it is almost impossible to directly identify glycoproteins without the preparation and pretreatment of samples.<sup>[2]</sup> Furthermore, biological samples, especially proteins, are damaged by this process. Therefore, the development of a nondestructive, facile, and highly sensitive method for glycoprotein analysis is of great importance.

Fluorescence methods have emerged as powerful techniques owing to their high sensitivity, fast response, and ability to afford high spatial resolution through microscopic imaging.<sup>[3a]</sup> Highly sensitive fluorescence detection methods have

been successfully used for cell imaging and protein analysis.<sup>[3b,c]</sup> To date, the strategy for the construction of fluorescence biosensing systems is the selection of suitable recognition elements and signal-transduction materials, which are then assembled together. Antibodies and enzymes are the most commonly used recognition elements for the design of biosensing systems,<sup>[3d]</sup> but they often suffer from low stability and high cost, which have limited their further application. Thus, chemically stable, low-cost artificial molecular-recognition materials are still in high demand.

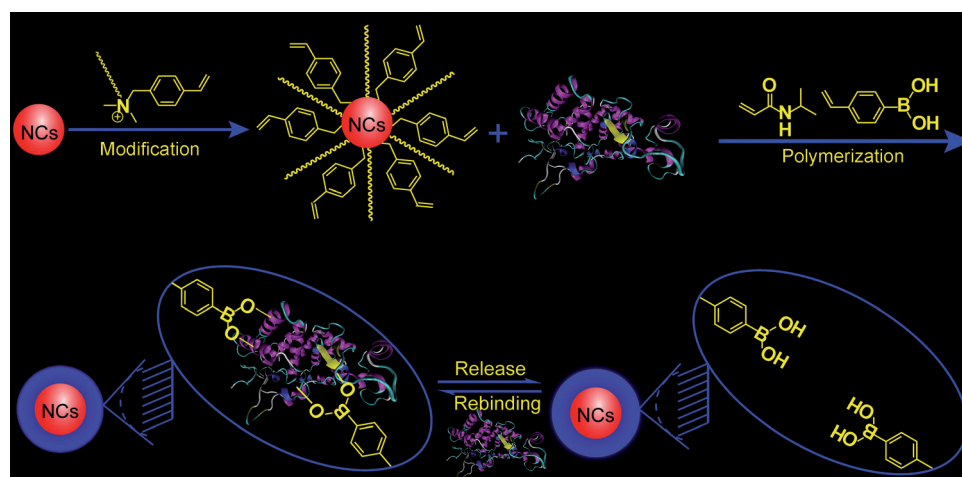
Molecularly imprinted polymers (MIPs) have been widely used as artificial receptors in the fields of antibody mimetics, chromatographic separation, and catalysis,<sup>[4–6]</sup> and recognition sites based on boronate affinity have gained attention owing to their reversible formation of covalent bonds with structures containing a *cis* diol in an alkaline aqueous solution.<sup>[7]</sup> We felt that a combination of the merits of MIPs and boronate affinity could enable the development of a new recognition element, which could lead to a higher specific binding capacity for glycoproteins through a synergistic effect. Furthermore, CdTe nanocrystals (NCs) have shown great potential as signal-transduction materials in chemical sensors because of their good photostability and high luminescence efficiency.<sup>[8]</sup> Therefore, we constructed a novel nanosensor based on spatial structure and boronic acid as recognition elements and NCs as a signal-transduction material. As far as we know, the use of a fluorescence nanosensor for glycoproteins has not been reported to date.

To fabricate the nanosensor, we coated the CdTe NCs with the new polymerizable surfactant octadecyl-*p*-vinylbenzyltrimethylammonium chloride (OVDAC) and copolymerized the OVDAC-coated CdTe with the monomers *N*-isopropylacrylamide (NIPAAm) and 4-vinylphenylboronic acid (VPBA) in the presence of the template glycoprotein (Scheme 1). The molecularly imprinted 3D network and boronic acid based recognition element give rise to a higher specific binding capacity for the target glycoprotein through a synergistic effect. NIPAAm was introduced as a temperature-sensitive element that allowed for swelling and shrinking with temperature, and the reversible interaction of VPBA with the glycoprotein was regulated by the pH value (Scheme 2). By using horseradish peroxidase (HRP) as a model target, we investigated the properties and performance of the prepared nanosensor as well as the regulation of the temperature and pH value. The generality of the method was demonstrated by the successful imprinting of two glycoproteins (HRP and ovalbumin). Moreover, the nanosensor was successfully applied to the detection of HRP in biological fluids. The

[\*] Dr. W. Zhang, W. Liu, Prof. P. Li, H. Xiao, Dr. H. Wang, Prof. B. Tang  
College of Chemistry, Chemical Engineering and Materials Science  
Collaborative Innovation Center of Functionalized Probes for  
Chemical Imaging in Universities of Shandong, Key Laboratory of  
Molecular and Nano Probes, Ministry of Education, Shandong  
Normal University  
Jinan 250014 (P.R. China)  
E-mail: tangb@sdsu.edu.cn

[\*\*] This research was supported by the 973 Program (2013CB933800),  
the National Natural Science Foundation of China (21227005,  
21390411, 91313302, 21035003, 21305080), the Natural Science  
Foundation of Shandong Province of China (ZR2013BQ005), and  
the Program for Changjiang Scholars and Innovative Research  
Teams in University.

Supporting information for this article is available on the WWW  
under <http://dx.doi.org/10.1002/anie.201405634>.



**Scheme 1.** Self-assembly of the NCs, the polymerizable surfactant OVDAC, and boronic acid and acryamide monomers for the preparation of a fluorescence nanosensor.

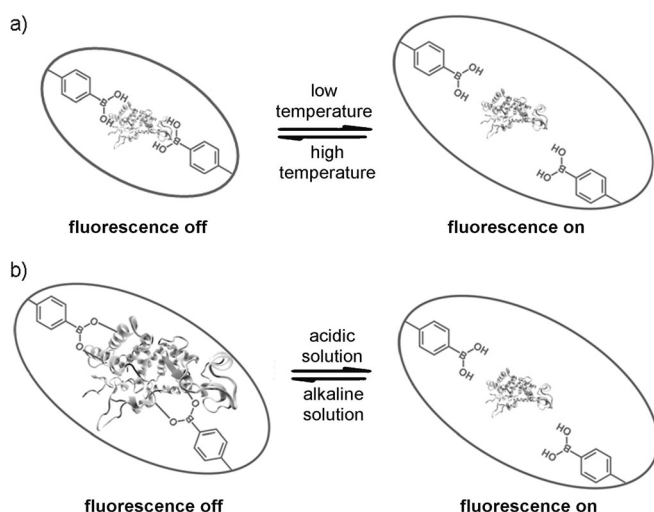
(Figure S1b), mainly as a result of the interaction between the NCs and OVDAC. Subsequently, the OVDAC-coated NCs, NIPAAm, VPBA, and the target glycoprotein were copolymerized to give a fluorescence nanosensor, and a glycoprotein MIP layer was thus produced on the surface of the NCs. Removal of the target molecules led to imprinted 3D cavities, and the as-prepared MIP-based nanosensor could be used for the selective recognition of the target glycoprotein.

TEM images of the MIP-based nanosensor and nonimprinted polymer (NIP; see

Figure S2 in the Supporting Information) showed that the MIP-based nanosensor had a uniform size of about 60 nm, and that the size and shape of the NIP were not distinctly different from those in the MIP-based nanosensor. Therefore, the different performance of the MIP-based nanosensor and the NIP in the subsequent study could be attributed to the imprinting effect, but not to a morphological difference between the MIP-based nanosensor and the NIP (see Figure S2 for photographs of the MIP-based nanosensor and the NIP under ultraviolet radiation). A small difference observed in the emission intensity of the MIP solution and the NIP solution is mainly due to the difference in the native structures of the MIP-based nanosensor and the NIP. All bands in the FTIR spectra of the NCs, the MIP-based nanosensor, and the NIP (see Figure S3) showed that the surface of the NCs was modified with pNIPAAm and VPBA. X-ray photoelectron spectroscopy (XPS) further indicated that VPBA and the MIP were grafted on the surface of the NCs (see Figure S4).

Thermosensitive polymers are well-known for swelling and shrinking reversibly with changes in temperature. To confirm the properties of the nanosensor, we carried out a temperature-response test (Figure 1). Figure 1a,b shows the fluorescence intensity of the MIP-based nanosensor with the target glycoprotein HRP as a function of temperature at 20 and 44 °C. The interaction of the MIP-based nanosensor with HRP showed conspicuous temperature-dependent on–off fluorescence intensity, which indicated the recognition ability of the MIP-based nanosensor upon changes in temperature (Scheme 2). The influence of the temperature on the adsorption of HRP was investigated (Figure 1c,d). The results showed that the swelling and shrinking states were associated with a change in temperature and the binding ability was associated with a change in the polymer volume.

The pH value is critical for the interaction of boronic acids with compounds containing a *cis* diol. On the basis of the mechanism of boronate affinity, boronic acids can form reversible covalent bonds with *cis*-diol-containing structures



**Scheme 2.** Proposed mechanism of the fluorescence nanosensor for the capture and release of the target glycoprotein through control of the temperature and pH value: a) swelling and shrinking of the imprinted cavities upon changes in temperature; b) reversible formation of covalent bonds between boronic acid moieties and the glycoprotein upon changes in the pH value.

present study provides a facile and efficient fluorescence tool for glycoprotein detection in clinical diagnostics.

The general scheme for the synthesis of the MIP-based nanosensor is illustrated in Scheme 1. First, the polymerizable surfactant OVDAC was used to replace surface ligands of the NCs. The electrostatic interaction between the negatively charged CdTe NCs and the positively charged surfactant OVDAC was the main driving force for the formation of the desired surface structure. To study the optical properties of OVDAC and the CdTe NCs, we investigated the fluorescence emission and UV/Vis absorption of OVDAC, the CdTe NCs, and the mixture of CdTe NCs with OVDAC. The fluorescence intensity of the CdTe NCs was quenched by OVDAC

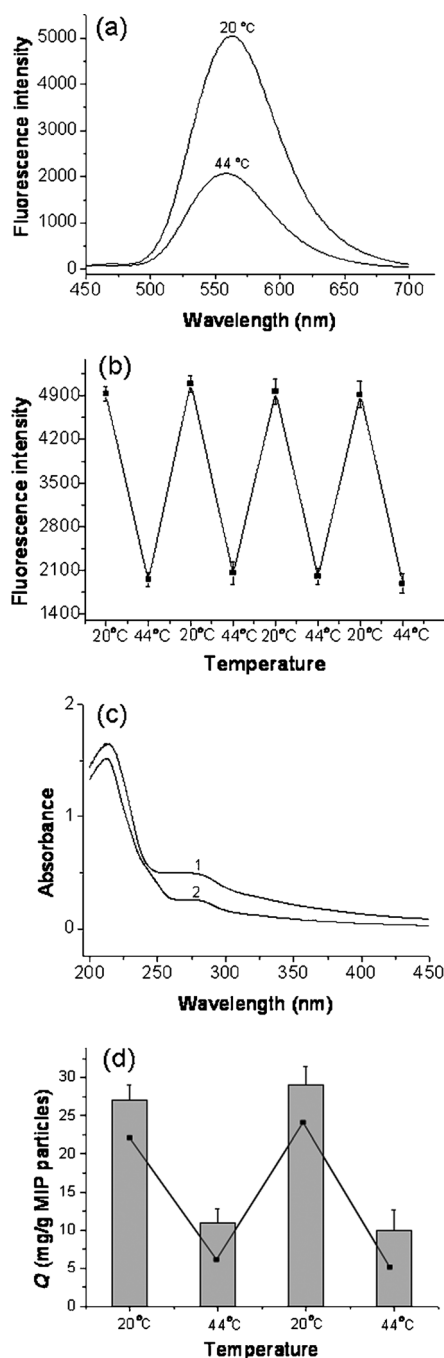


**Figure 1.** a,b) Changes in the fluorescence intensity of the MIP-based nanosensor for the template HRP with a temperature swing between 20 and 44 °C; c) UV/Vis spectra of the HRP solution before (curve 1) and after adsorption by the MIP-based nanosensor (curve 2); d) adsorption capacity of the MIP-based nanosensor for the template HRP at 20 and 44 °C. Experimental conditions: a)  $c_{\text{HRP}} = 10 \mu\text{g mL}^{-1}$ ,  $c_{\text{MIP}} = 20 \mu\text{g mL}^{-1}$ ; b) a solution of HRP ( $0.2 \text{ mg mL}^{-1}$ , 2.0 mL) was incubated with the MIP-based nanosensor (20 mg). The error bars were calculated from three parallel experiments.

within the alkaline pH range, whereas the reversible covalent bond dissociates when the medium becomes acidic (Scheme 2). This behavior is an apparent advantage for boronate-affinity-related imprinted materials: Template removal is more efficient owing to the boronate-affinity

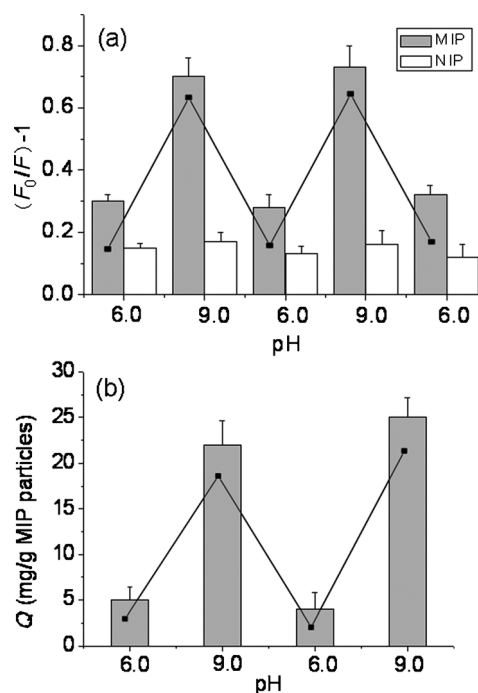


**Figure 2.** a) Changes in the fluorescence intensity of the MIP-based nanosensor and the NIP in the presence of the glycoprotein HRP at pH 6.0 and 9.0; b) adsorption capacity of the MIP-based probe for the template HRP at pH 6.0 and 9.0. Experimental conditions: a)  $c_{\text{MIP}} = c_{\text{NIP}} = 20 \mu\text{g mL}^{-1}$ ,  $c_{\text{HRP}} = 10 \mu\text{g mL}^{-1}$ ; b) a solution of HRP ( $0.2 \text{ mg mL}^{-1}$ , 2.0 mL) was incubated with the MIP-based probe (20 mg). The error bars were calculated from three parallel experiments.

interaction between template glycoproteins, and boronic acid ligands can be destroyed readily by the use of an acidic solution. The effect of the pH value on recognition performance was examined (Figure 2). Figure 2a shows the specific binding capability of the HRP-imprinted MIP-based nanosensor and the NIP at pH 6.0 and 9.0. The NIP exhibited a very limited change in fluorescence, whereas the MIP-based nanosensor exhibited a larger change in fluorescence at pH 9.0 than that at pH 6.0. We investigated the influence of the pH value on the adsorption of HRP (Figure 2b) and found that the binding ability was associated with the pH value. This result is consistent with the stabilization of the interaction between the boronic acid and *cis*-diol moieties at higher pH values. Moreover, the general applicability of the approach was demonstrated by the use of different template molecules (ovalbumin; see Figure S5). Thus, the boronate-affinity-based nanosensor holds great potential for the detection of target glycoproteins in real samples.

The binding performance of the MIP-based nanosensor was studied on the basis of changes in the fluorescence signal (Figure 3). The fluorescence intensity of the MIP-based nanosensor was quenched gradually as the concentration of the HRP target increased, mainly as a result of an adsorptive affinity interaction between the nanosensor and the target glycoprotein. The imprinted cavities and the spatial orientation of the functional groups were established in the process of imprinting. For the MIP-based nanosensor, the fluores-

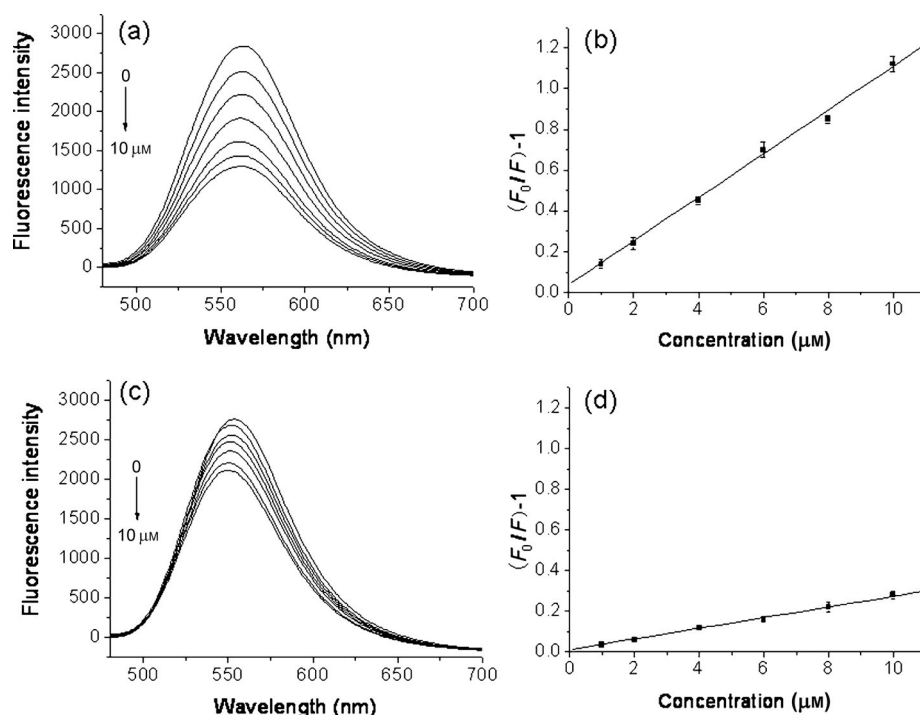


**Figure 3.** a,c) Fluorescence emission spectra of the MIP-based nanosensor (a) and the NIP (c) upon the addition of a solution of the target glycoprotein HRP at the indicated concentration. b,d) Stern–Volmer plots for the MIP-based nanosensor (b) and the NIP (d) with the target glycoprotein HRP.  $c_{\text{MIP}} = c_{\text{NIP}} = 20 \mu\text{g mL}^{-1}$ . The error bars were calculated from three parallel experiments.

cence quenching was mainly due the specific affinity interaction of the imprinted cavities with the target glycoprotein. The imprinting factor (IF), which is the ratio of  $K_{\text{SV,MIP}}$  and  $K_{\text{SV,NIP}}$  ( $K_{\text{SV,MIP}}$  and  $K_{\text{SV,NIP}}$  are the linear slopes in Figure 3 b,d, respectively), was used to evaluate the selectivity of the nanosensor. Under the optimal conditions, the IF value ( $K_{\text{SV,MIP}}/K_{\text{SV,NIP}}$ ) was 3.83, which suggests that the MIP-based nanosensor can enhance the quenching efficiency of fluorescence intensity, thus enlarging the spectral sensitivity of the MIP-based nanosensor for the target glycoprotein. Figure 3b,d was plotted on the basis of the Stern–Volmer equation for the MIP-based nanosensor and the NIP, respectively, in the presence of the glycoprotein:

$$F_0/F = 1 + K_{\text{SV}} [Q] \quad (1)$$

$F_0$  and  $F$  are the fluorescence intensity of the nanosensor in the absence and presence of the template, respectively;  $K_{\text{SV}}$  is the Stern–Volmer constant, and  $[Q]$  is the quencher concentration.

The specificity of the MIP-based nanosensor was further investigated. A series of single and binary protein solutions of HRP–BSA were used to show the specific recognition ability of the nanosensor (see Figure S6 and Table S1). Each type of imprinted sensor exhibited specific affinity adsorption of the target glycoprotein in the presence of structurally related proteins, thus clearly demonstrating that the imprinted sensors displayed selectivity for the target glycoprotein and exhibited lower cross-reactivity with structurally related proteins. The results also demonstrated that the molecularly

imprinted spatial structure discriminated proteins on the basis of molecular shape rather than size. Competitive experiments in the presence of sugars (D-fructose; see Figures S7 and S8) showed that this recognition is indeed based on a synergistic effect of the glycosyl groups and molecular imprinting. Finally, the developed MIP-based nanosensor was employed for the selective detection of HRP in biological fluids, such as urine samples. An appropriate (100-fold) diluted solution of human urine spiked with HRP was found to be sufficient for the quantitative recovery of HRP (Table 1).

In conclusion, a novel glycoprotein nanosensor combining the merits of a molecularly imprinted spatial structure and boronate affinity has been synthesized and applied for the selective monitoring of glycoproteins. The multiple recognition ability based on the spatial structure of the MIP and boronic acid recognition sites led to higher

**Table 1:** Results for the quantitative detection of HRP in human urine.

Sample	HRP concentration [ $\times 10^{-6}$ M] spiked	Amount detected [%] <sup>[a]</sup>
1	0.0	n.d. <sup>[b]</sup>
1	2.0	105.0 $\pm$ 5.0
1	5.0	98.0 $\pm$ 6.0
2	0.0	n.d. <sup>[b]</sup>
2	5.0	102.0 $\pm$ 4.0
2	10.0	97.0 $\pm$ 3.0

[a] The mean  $\pm$  the standard deviation for three experiments is given.

[b] Not detected.

a specific binding capacity for the glycoprotein through a synergistic effect. CdTe NCs were selected for their excellent optical properties as fluorescent signal-transduction materials to enable the facile and highly sensitive detection of glycoproteins. Moreover, the recognition performance of the nanosensor for the target glycoprotein was regulated by controlling the pH value and temperature. The nanosensor was successfully applied in the detection of HRP in biological fluids. We believe that this strategy for the construction of nanosensors will be broadly applicable to the quantitative detection of glycoproteins in biological systems.

Received: May 30, 2014

Revised: August 9, 2014

Published online: September 11, 2014



**Keywords:** artificial receptors · boronate affinity · fluorescence nanosensors · glycoproteins · molecular recognition

- [1] a) B. S. Ireland, U. Brockmeier, C. M. Howe, T. Elliott, D. B. Williams, *Mol. Biol. Cell* **2008**, *19*, 2413–2423; b) K. Ohtsubo, J. D. Marth, *Cell* **2006**, *126*, 855–867; c) L. Krishnamoorthy, L. K. Mahal, *ACS Chem. Biol.* **2009**, *4*, 715–732.
- [2] a) S. Nie, A. Lo, J. Zhu, J. Wu, M. T. Ruffin, D. M. Lubman, *Anal. Chem.* **2013**, *85*, 5353–5357; b) H. N. Behnken, A. Ruthenbeck, J. M. Schulz, B. Meyer, *J. Proteome Res.* **2014**, *13*, 997–1001; c) W. R. Alley, Jr., B. F. Mann, M. V. Novotny, *Chem. Rev.* **2013**, *113*, 2668–2732.
- [3] a) Y. Urano, M. Kamiya, K. Kanda, T. Ueno, K. Hirose, T. Nagano, *J. Am. Chem. Soc.* **2005**, *127*, 4888–4894; b) M. Lowry, S. O. Fakayode, M. L. Geng, G. A. Baker, L. Wang, M. E. McCarroll, G. Patonay, I. M. Warner, *Anal. Chem.* **2008**, *80*, 4551–4574; c) J. Chan, S. C. Dodani, C. J. Chang, *Nat. Chem.* **2012**, *4*, 973–984; d) T. Ozawa, H. Yoshimura, S. B. Kim, *Anal. Chem.* **2013**, *85*, 590–609.
- [4] a) H. Shi, W. Tsai, M. D. Garrison, S. Ferrari, B. D. Ratner, *Nature* **1999**, *398*, 593–597; b) T. Miyata, M. Jige, T. Nakaminami, T. Uragami, *Proc. Natl. Acad. Sci. USA* **2006**, *103*, 1190–1193; c) A. Bossi, S. A. Piletsky, E. V. Piletska, P. G. Righetti, A. P. F. Turner, *Anal. Chem.* **2001**, *73*, 5281–5286; d) K. Haupt, *Nat. Mater.* **2010**, *9*, 612–614.
- [5] a) L. Ye, K. Mosbach, *J. Am. Chem. Soc.* **2001**, *123*, 2901–2902; b) H. F. Wang, Y. He, T. R. Ji, X. P. Yan, *Anal. Chem.* **2009**, *81*, 1615–1621; c) H. H. Yang, S. Q. Zhang, W. Yang, X. L. Chen, Z. X. Zhuang, J. G. Xu, X. R. Wang, *J. Am. Chem. Soc.* **2004**, *126*, 4054–4055; d) Y. Ma, G. Q. Pan, Y. Zhang, X. Guo, H. Q. Zhang, *Angew. Chem. Int. Ed.* **2013**, *52*, 1511–1514; *Angew. Chem.* **2013**, *125*, 1551–1554; e) Y. Hoshino, H. Koide, T. Urakami, H. Kanazawa, T. Kodama, N. Oku, K. J. Shea, *J. Am. Chem. Soc.* **2010**, *132*, 6644–6645; f) A. Cumbo, B. Lorber, P. F. X. Corvini, W. Meier, P. Shahgaldian, *Nat. Commun.* **2013**, *4*, 1503–1509.
- [6] a) W. Wan, M. Biyikal, R. Wagner, B. Sellergren, K. Rurack, *Angew. Chem. Int. Ed.* **2013**, *52*, 7023–7027; *Angew. Chem.* **2013**, *125*, 7161–7165; b) R. Wagner, W. Wan, M. Biyikal, E. Benito-Peña, M. C. Moreno-Bondí, I. Lazraq, K. Rurack, B. Sellergren, *J. Org. Chem.* **2013**, *78*, 1377–1389; c) R. Martínez-Máñez, F. Sancenón, M. Biyikal, M. Hecht, K. Rurack, *J. Mater. Chem.* **2011**, *21*, 12588–12604; d) A. Nematollahzadeh, W. Sun, C. S. A. Aureliano, D. Luetkemeyer, J. Stute, M. J. Abdekhodaie, A. Shojaei, B. Sellergren, *Angew. Chem. Int. Ed.* **2011**, *50*, 495–498; *Angew. Chem.* **2011**, *123*, 515–518; e) J. Tan, H. Wang, X. Yan, *Anal. Chem.* **2009**, *81*, 5273–5280; f) L. Li, Y. Lu, Z. Bie, H. Chen, Z. Liu, *Angew. Chem. Int. Ed.* **2013**, *52*, 7451–7454; *Angew. Chem.* **2013**, *125*, 7599–7602.
- [7] a) Y. C. Liu, Y. Lu, Z. Liu, *Chem. Sci.* **2012**, *3*, 1467–1471; b) L. B. Ren, Z. Liu, Y. C. Liu, P. Dou, H. Y. Chen, *Angew. Chem. Int. Ed.* **2009**, *48*, 6704–6707; *Angew. Chem.* **2009**, *121*, 6832–6835; c) Z. Lin, L. Sun, W. Liu, Z. Xia, H. Yang, G. Chen, *J. Mater. Chem. B* **2014**, *2*, 637–643; d) A. E. Gregory, J. P. Michael, T. R. Ronald, *J. Am. Chem. Soc.* **2012**, *134*, 3631–3634.
- [8] a) W. C. W. Chan, S. Nie, *Science* **1998**, *281*, 2016–2018; b) X. Michalet, F. F. Pinaud, L. A. Bentolila, J. M. Tsay, S. Doose, J. J. Li, G. Sundaresan, A. M. Wu, S. S. Gambhir, S. Weiss, *Science* **2005**, *307*, 538–544.